JOURNAL OF GUIDANCE, CONTROL, AND DYNAMICS
Vol. 34, No. 4, July–August 2011

Feedback Control with Nominal Inputs for Agile Satellites Using Control Moment Gyros

Y. Kusuda* and M. Takahashi†
Keio University, Kanagawa 223-8522, Japan

DOI: 10.2514/1.49410

Satellites orbiting the Earth require large-angle and rapid rotational maneuverability. Control moment gyros are expected to be applied to attitude control actuators of small agile satellites, because control moment gyros can generate high torque effectively. However, the control moment gyro has a singularity problem that affects its energy consumption and rapid actuation. To solve the problem, a feedforward control logic using an energy-optimal path planned by a Fourier basis algorithm is proposed here. However, this logic alone cannot maintain precise control under actual errors and disturbances. Therefore, a feedback control system was also designed in order to acquire robustness against errors and disturbances. The designed system included in this paper is characterized by using a system's limit state, which is a newly defined variable, and is predicted by numerical integrals using nominal control inputs. Several numerical simulations and experiments were carried out to verify the feasibility of the proposed logic in terms of the robustness, energy consumption, and the safe use of the control moment gyro.

Nomenclature

b	=	skew angle of four control moment gyros, rad
$\mathbf{E}$	=	Fourier base term matrix
$\mathbf{H}_B$	=	total angular momentum vector, kgm^2/s
$\mathbf{h}$	=	angular momentum vector of four control moment gyros, kgm^2/s
h_{CMG}	=	angular momentum of control moment gyro wheel, kgm^2/s
$\mathbf{I}$	=	satellite inertia matrix, kgm^2
$\mathbf{I}_0$	=	unit matrix
J	=	evaluation function of path planning
$\mathbf{q}$	=	quaternion vector
$\mathbf{T}_i$	=	output torque vector of ith control moment gyro, Nm
$\mathbf{u}$	=	control input vector
$\mathbf{u}_{\mathrm{nom}}$	=	nominal control input vector
$\mathbf{x}$	=	state variable vector
$\mathbf{x}_d$	=	reference state variable vector
$\mathbf{x}_{\mathrm{pre}}$	=	system's limit state variable vector
$\boldsymbol{\alpha}$	=	Fourier series vector
$\boldsymbol{\delta}$	=	control moment gyro gimbal angle vector, rad
$\dot{\boldsymbol{\delta}}$	=	control moment gyro gimbal angular velocity vector, rad/s
$\boldsymbol{\omega}$	=	satellite angular velocity vector, rad/s

I. Introduction

THE demand for Earth observation satellites equipped with high-performance observing sensors has increased recently in order to acquire high-resolution images of specific ground targets. To achieve the precise observation, the satellites will turn rapidly rather than sweep the imaging system from side to side because pointing the whole body at the target allows the imaging system to achieve higher definition and to improve the resolution of its images. Moreover, the cost and effectiveness of such agile satellites are greatly affected by the average maneuvering time and observing frequency. Therefore, an attitude control system of such agile satellites requires the development of large-angle rapid rotational maneuverability [1].

To achieve the rapid rotational maneuver, control moment gyros (CMGs), not reaction wheels, are expected to be used as attitude control actuators of agile satellites, because the CMGs can effectively generate higher torque than reaction wheels. In this paper, it is assumed that the agile satellite equips a pyramid arrangement of four single-gimbal CMGs shown in Fig. 1 for a three-axis attitude control. Figure 2 shows a block diagram of an existing control system using a CMG steering logic. This is based on a distributive property from three-axis attitude control torques to four CMGs control inputs. However, there is a problem that a dimension of output torques degenerates from three dimensions to two dimensions or less, depending on CMG gimbal angles. The problem is called a singularity problem. At the singularity state, an output torque along a particular direction cannot be generated. In this condition, the CMG system cannot fulfill the requirement of the rapid maneuverability. Therefore, several CMG singularity avoidance steering logics have been proposed so far. For example, there is the generalized singularity robust inverse (GSRInverse) method [2], singularity direction avoidance method [3], and so on [4–6].

In the existing control logics, there is a problem that a rapid actuation is needed to avoid the singularity state. Such an actuation has a possibility of causing the breakdown of the CMG. This problem is related to the subsistence of the entire satellite system. To achieve the safe use of the CMG, the objective of the controller design is to control the CMG smoothly with keeping maximum angular velocities low and avoiding vibrating motions. Moreover, in these logics, there is a problem of not considering the CMG energy consumption. As long as the control systems are separated into an attitude control system and a CMG steering logic, the optimality about the whole control system cannot be evaluated with respect to the energy consumption. Therefore, it is believed that the optimality about the energy consumption should be evaluated as a whole system without a CMG steering logic.

To deal with these problems, a feedforward control logic using CMG optimal paths by Fourier basis algorithm (FBA) is designed in consideration of the CMG energy consumption under a control requirement [7]. Several numerical simulations indicate the effectiveness of the proposed logic in terms of the energy consumption and the safe use of the CMG by comparing with the existing control logic.

In an actual implementation, there are several disturbances and errors that cannot be assumed in the path planning. Under the disturbances and errors, the proposed logic cannot achieve a high-precision control because the proposed logic does not have a

Presented as Paper 2009-6205 at the AIAA Guidance, Navigation, and Control Conference, Chicago, IL, 10–13 August 2009; received 17 February 2010; revision received 15 January 2011; accepted for publication 25 January 2011.

*Graduate Student, Department of System Design Engineering, 3-14-1 Hiyoshi, Kohoku-ku, Yokohama-shi; kusuda@yt.sd.keio.ac.jp.

†Associate Professor, Department of System Design Engineering, 3-14-1 Hiyoshi, Kohoku-ku, Yokohama-shi; takahashi@sd.keio.ac.jp.

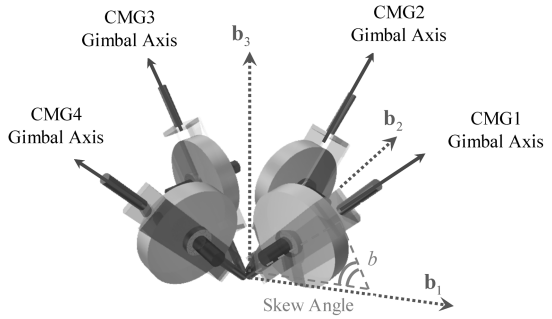

Fig. 1 Pyramid arrangement of four single-gimbal CMGs.

feedback controller. If a maneuver has initial errors, the proposed feedforward control system has a risk of increasing terminal state errors. Because CMGs has a strong nonlinearity, when a feedforward controller is combined with a stationary linear feedback controller, the satellite attitude cannot be controlled to the reference attitude.

From the background, the purpose of this paper is to design a feedback control system with nominal inputs shown in Fig. 3 so as to compensate for errors and disturbances. The designed feedback control system is based on the system's limit state feedback control logic [8]. This logic uses a system's limit state, which is a terminal state variable predicted by numerical integrals. Though it is generally difficult to control the nonlinear system, the reachability to a reference state can be ensured by using the prediction and combining the paths that have been planned as nominal inputs.

In this paper, the feasibility about the robustness of the designed control system was verified by an original CMG experimental setup. Furthermore, the experiments indicate the effectiveness of the proposed logic for the energy consumption and the safe use of the CMG in comparison with the existing logic.

II. Formulation of Satellite Attitude Maneuver Using CMG

A. Mathematical Modeling

In this paper, an agile satellite has a CMG system that is a pyramid arrangement of four single-gimbal CMGs in Fig. 1. This section describes fundamental principles of rigid satellite rotational equations and CMG dynamics. The objective of this section is to construct a numerical calculation model of the satellite attitude maneuver using the CMGs. Because the mission is a large-angle rapid maneuver, the expression of the satellite attitude is the following quaternion kinematics equation:

$$\dot{\mathbf{q}} = \frac{1}{2}\begin{bmatrix} 0 & \omega_3 & -\omega_2 & \omega_1 \\ -\omega_3 & 0 & \omega_1 & \omega_2 \\ \omega_2 & -\omega_1 & 0 & \omega_3 \\ -\omega_1 & -\omega_2 & -\omega_3 & 0 \end{bmatrix}\mathbf{q} = \bar{\boldsymbol{\omega}} \cdot \mathbf{q} \tag{1}$$

where $\mathbf{q} = (q_1, q_2, q_3, q_4)^T$ is a quaternion vector, $\boldsymbol{\omega} = (\omega_1, \omega_2, \omega_3)^T$ is a satellite angular velocity vector, and $\bar{\boldsymbol{\omega}}$ is a matrix of a satellite angular velocity. The quaternion has the following constraint equation $q_1^2 + q_2^2 + q_3^2 + q_4^2 = 1$.

From the principle of the angular momentum conservation, an equation of the rotational motion of a rigid satellite equipped with the CMG is given by the following equation:

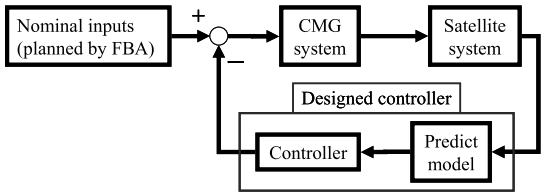

Fig. 3 Block diagram of the proposed control system.

$$\frac{\mathrm{d}\mathbf{H}_B}{\mathrm{d}t} + \boldsymbol{\omega} \times \mathbf{H}_B = \mathbf{0} \tag{2}$$

where $\mathbf{H}_B$ is a total angular momentum vector expressed in the satellite body-fixed control axes. External torques, such as natural environmental torques, can be regarded as zero during a short-time rapid maneuver.

The total angular momentum vector consists of the satellite main body angular momentum and the CMG angular momentum:

$$\mathbf{H}_B = \mathbf{I}\boldsymbol{\omega} + \mathbf{h} \tag{3}$$

where $\mathbf{I}$ is a satellite inertia matrix and $\mathbf{h}$ is a CMG angular momentum vector expressed in the satellite body-fixed control axes.

When Eq. (3) is substituted into Eq. (2), this equation is given by

$$\mathbf{I}\,\dot{\boldsymbol{\omega}} + \boldsymbol{\omega} \times \mathbf{I}\boldsymbol{\omega} + \dot{\mathbf{h}} + \boldsymbol{\omega} \times \mathbf{h} = \mathbf{0} \tag{4}$$

where Eq. (4) is a rotation dynamic equation and $\dot{\mathbf{h}}$ is a time-derivation vector of the CMG angular momentum. The satellite attitude can be controlled by changing a direction of the CMG angular momentum.

The angular momentum of the skew-type four CMGs expressed in Fig. 1 is a function depending on the gimbal angles $\boldsymbol{\delta} = (\delta_1, \delta_2, \delta_3, \delta_4)^T$ as follows:

$$\mathbf{h} = h_{\mathrm{CMG}}\begin{bmatrix} -cb\sin\delta_1 - \cos\delta_2 + cb\sin\delta_3 + \cos\delta_4 \\ \cos\delta_1 - cb\sin\delta_2 - \cos\delta_3 + cb\sin\delta_4 \\ sb\sin\delta_1 + sb\sin\delta_2 + sb\sin\delta_3 + sb\sin\delta_4 \end{bmatrix} \tag{5}$$

where b is an inclination angle of a CMG gimbal axis in Fig. 1, that is called a skew angle. $sb \equiv \sin b$, $cb \equiv \cos b$, and h_{CMG} is a CMG wheel angular momentum. A time derivative of the CMG angular momentum vector can be obtained as

$$\begin{aligned}\dot{\mathbf{h}} &= h_{\mathrm{CMG}}\begin{bmatrix} -cb\cos\delta_1 & \sin\delta_2 & cb\cos\delta_3 & -\sin\delta_4 \\ -\sin\delta_1 & -cb\cos\delta_2 & \sin\delta_3 & cb\cos\delta_4 \\ sb\cos\delta_1 & sb\cos\delta_2 & sb\cos\delta_3 & sb\cos\delta_4 \end{bmatrix}\dot{\boldsymbol{\delta}} \\ &= \mathbf{A}(\boldsymbol{\delta})\dot{\boldsymbol{\delta}}\end{aligned} \tag{6}$$

where $\dot{\boldsymbol{\delta}} = (\dot{\delta}_1, \dot{\delta}_2, \dot{\delta}_3, \dot{\delta}_4)^T$ is a CMG gimbal angular velocity vector and $\mathbf{A}$ is a 3×4 Jacobian matrix. One approach of designing CMG steering logics involves the differential relation. Consequently, the mathematical model of the satellite attitude maneuver using the CMG is described by

$$\begin{bmatrix} \dot{\mathbf{q}} \\ \dot{\boldsymbol{\omega}} \end{bmatrix} = \begin{bmatrix} \bar{\boldsymbol{\omega}}\mathbf{q} \\ -\mathbf{I}^{-1}(\boldsymbol{\omega} \times \mathbf{I}\boldsymbol{\omega} + \boldsymbol{\omega} \times \mathbf{h}(\boldsymbol{\delta})) \end{bmatrix} + \begin{bmatrix} \mathbf{0} \\ -\mathbf{I}^{-1}\mathbf{A}(\boldsymbol{\delta}) \end{bmatrix}\dot{\boldsymbol{\delta}} \tag{7}$$

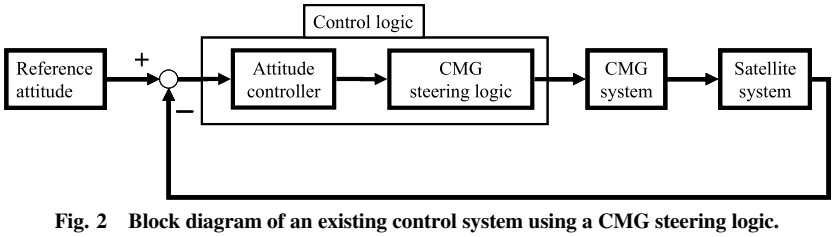

Fig. 2 Block diagram of an existing control system using a CMG steering logic.

$$\dot{\mathbf{x}} = \mathbf{g}(\mathbf{x}, \boldsymbol{\delta}) + \mathbf{f}(\mathbf{x}, \boldsymbol{\delta})\mathbf{u} \tag{8}$$

where $\mathbf{x}$ is a state variable vector that consists of the quaternion vector $\mathbf{q}$ and the satellite angular velocity vector $\boldsymbol{\omega}$. A control input vector $\mathbf{u}$ is the CMG gimbal angular velocity vector $\dot{\boldsymbol{\delta}}$.

B. CMG Steering Logic

For a simple satellite model, one can design an attitude control system and a CMG momentum management system on the basis of Eqs. (6) and (7). One approach involves the differential relation between the gimbal angles and the CMG angular momentum vector. The design of the CMG steering logics, which generate the CMG gimbal angular velocity commands, focuses on finding an inverse of $\dot{\mathbf{h}} = \mathbf{A}(\boldsymbol{\delta})\dot{\boldsymbol{\delta}}$. Here, a GSRInverse steering logic [2] is briefly shown as a comparative control system.

The GSRInverse steering logic can be represented as

$$\dot{\boldsymbol{\delta}} = \mathbf{A}^{\#}\boldsymbol{\tau} \tag{9}$$

$$\mathbf{A}^{\#} = \mathbf{A}^T[\mathbf{A}\mathbf{A}^T + \lambda\mathbf{B}]^{-1} \tag{10}$$

$$\mathbf{B} = \begin{bmatrix} 1 & \varepsilon_3 & \varepsilon_2 \\ \varepsilon_3 & 1 & \varepsilon_1 \\ \varepsilon_2 & \varepsilon_1 & 1 \end{bmatrix} > 0 \tag{11}$$

$$\lambda = \begin{cases} 0 & \text{for } m \geq m_0 \\ \lambda_0(1 - m/m_0)^2 & \text{for } m \leq m_0 \end{cases} \tag{12}$$

where $\boldsymbol{\tau}$ is a vector of commanded satellite control torques, $\varepsilon_i = \varepsilon_0 \sin(\omega_s t + \phi_i)$ and $m = \sqrt{\det(\mathbf{A}\mathbf{A}^T)}$. The scalar $\lambda_0, m_0, \varepsilon_0, \omega_s$ and ϕ_i need to be appropriately selected. The GSRInverse steering logic is based on the mixed, two-norm and weighted least-squares minimization. The logic regularly works as effectively as the basic pseudoinverse steering logic $\mathbf{A}^{\#} = \mathbf{A}^T[\mathbf{A}\mathbf{A}^T]^{-1}$ and, near the singularity state, this logic works to avoid the singularity state by the newly added term $\lambda\mathbf{B}$.

III. Control System Design

A. Path Planning by Fourier Basis Algorithm

1. Introduction

The purpose of the proposed logic is to control the system for the energy consumption and the safe use of the CMG without separating the whole control system into an attitude control system and a CMG control system. Therefore, a feedforward control system is designed on the basis of the path planning of control inputs, which are CMG gimbal angular velocities. In a real-time implementation, this path planning can be executed before the maneuver in order to use the unperformed time on the other side of the ground targets for the calculation time. The problem involving the energy consumption of CMG can be solved by considering it at the path planning. Moreover, the problem involving the rapid actuation of CMG also can be solved by applying the Fourier series approximation of control inputs to the path planning. This is because the rapid actuation occurs when a CMG steering logic works for avoiding the singularity state.

The method used for the path planning is the FBA [8–10], which is based on the approximation of the control inputs by using a Fourier series. This method is advantageous in terms of the calculation time of the path planning because there are fewer optimal parameters in FBA than in other methods that uses discrete-time control inputs. Additionally the control inputs approximated by the continuous function are predictably effective in smooth actuation. In the following section, a detailed explanation of the FBA is given.

2. Fourier Basis Algorithm

FBA is based on Fourier series approximation of control inputs. Newton method is applied to the optimization method in order to search for optimal Fourier parameters [7–10]. In this problem, the constraint condition is the motion equation shown in Eq. (7) and the boundary conditions of the state variables are described by

$$\mathbf{x}(0) = \mathbf{x}_0, \qquad \mathbf{x}(t_f) = \mathbf{x}_d \tag{13}$$

where $\mathbf{x}_0$ is an initial state variable vector and $\mathbf{x}_d$ is a terminal state variable vector. To satisfy the boundary conditions with keeping the energy consumption of the CMG low, the evaluation function of this optimization problem is set up as follows:

$$J(\mathbf{u}) = \int_0^{t_f} (\mathbf{u}(t)^T\mathbf{u}(t))\,\mathrm{d}t + (\mathbf{x}(t_f) - \mathbf{x}_d)^T\mathbf{M}(\mathbf{x}(t_f) - \mathbf{x}_d) \tag{14}$$

where t_f is a terminal time of the maneuver. The evaluation function is composed of the CMG control input norm $\mathbf{u}(t)^T\mathbf{u}(t)$, the state variables at the end of the maneuver, and the weighting matrix $\mathbf{M}$. The matrix must be large enough to satisfy the control requirement because the errors of the terminal states depend on the matrix $\mathbf{M}$. FBA approximates the control inputs by the Fourier series in order to search for the optimal path that minimizes the evaluation function under the control requirement:

$$\mathbf{u} = \mathbf{E}\boldsymbol{\alpha} \tag{15}$$

$$\begin{aligned}\mathbf{E} = [&\tfrac{1}{2}\mathbf{I}_0 \quad \mathbf{I}_0 \sin\omega_0 t \quad \mathbf{I}_0 \sin 2\omega_0 t \quad \cdots \\ &\mathbf{I}_0 \cos\omega_0 t \quad \mathbf{I}_0 \cos 2\omega_0 t \quad \cdots]\end{aligned} \tag{16}$$

where $\mathbf{E}$ is a Fourier base term matrix, $\boldsymbol{\alpha}$ is a Fourier coefficient parameter vector, $\mathbf{I}_0$ is a unit matrix, and ω_0 is a basic frequency of the Fourier series approximation. When the Fourier series approximation is set up to the N-order term and Eq. (15) is substituted into Eq. (14), the evaluation function Eq. (14) comes to depend on the Fourier parameters on the basis of orthogonality of trigonometric functions as follows:

$$J(\boldsymbol{\alpha}) = \boldsymbol{\alpha}^T\boldsymbol{\alpha} + (\mathbf{x}(t_f) - \mathbf{x}_d)^T\mathbf{M}(\mathbf{x}(t_f) - \mathbf{x}_d) \tag{17}$$

To obtain the optimal parameters that minimize the evaluation function, the Newton method is used as the searching algorithm [7–10]. This is because the Newton method is based on the first and second-order derivatives of the evaluation function and is superior in terms of the convergence property in obtaining the optimal solution. In general, the optimal solution using this method is said to have a property that is dependent on the initial condition. The optimal solution solved by using the Newton method is closer to a local optimal solution than to a global optimal solution. However, in this paper, this solution is regarded as an energy-optimal solution because the initial condition of the optimization is always set to $\mathbf{0}$, which means that the optimization must start at the initial condition that minimizes the energy consumption.

Next, the solution by the Newton method is described. The evaluation function in Eq. (17) can be Taylor-expanded around the present value of the optimal parameter $\boldsymbol{\alpha}_s$ as follows:

$$\begin{aligned}J(\boldsymbol{\alpha}_s + \Delta\boldsymbol{\alpha}) = J(\boldsymbol{\alpha}_s) &+ \frac{\partial J(\boldsymbol{\alpha}_s)}{\partial\boldsymbol{\alpha}}\Delta\boldsymbol{\alpha} \\ &+ \frac{1}{2}\left(\Delta\boldsymbol{\alpha}^T\frac{\partial^2 J(\boldsymbol{\alpha}_s)}{\partial\boldsymbol{\alpha}^T\partial\boldsymbol{\alpha}}\right)\Delta\boldsymbol{\alpha} + \mathbf{O}(\Delta\boldsymbol{\alpha}^3)\end{aligned} \tag{18}$$

where $\Delta\boldsymbol{\alpha}$ is a variation of Fourier parameters. Then $\Delta\boldsymbol{\alpha}$ is determined on the basis of the Newton method to satisfy $J(\boldsymbol{\alpha}_s + \Delta\boldsymbol{\alpha}) - J(\boldsymbol{\alpha}_s) < 0$ as follows:

$$\Delta\boldsymbol{\alpha} = -\mu(\mathbf{I}_0 + \mathbf{y}(t_f)^T\mathbf{M}\mathbf{y}(t_f))^{-1}(\boldsymbol{\alpha}_s + \mathbf{y}(t_f)^T\mathbf{M}(\mathbf{x}(t_f) - \mathbf{x}_d)) \tag{19}$$

where μ is a weighting constant to be properly selected, and $\mathbf{y}(t_f)$ is given by

$$\mathbf{y} = \frac{\partial\mathbf{x}}{\partial\boldsymbol{\alpha}} \tag{20}$$

$$\frac{\partial \mathbf{y}}{\partial t} = \left(\frac{\partial \mathbf{g}}{\partial \mathbf{x}} + \sum_{i=1}^{n}\left(\frac{\partial \mathbf{h}_i}{\partial \mathbf{x}} u_i\right)\right)\mathbf{y} + \mathbf{hE} \tag{21}$$

where the terminal value of $\mathbf{y}$ can be obtained by integrating Eqs. (20) and (21) in the numerical simulation.

Eventually, the updating equation of the Fourier parameters is as follows:

$$\boldsymbol{\alpha} = \boldsymbol{\alpha}_s + \Delta\boldsymbol{\alpha} \tag{22}$$

In this way, FBA can obtain the energy-optimal paths of the CMG control inputs.

3. Design of Evaluation Function

The basic evaluation function of the FBA estimates the energy consumption by the norm of control inputs. Then the energy consumption of the CMG cannot be estimated precisely because satellite angular velocities cannot be ignored with respect to CMG gimbal angular velocities in agile maneuvers. Therefore, in order to carefully evaluate the energy consumption of the CMG, the first term of Eq. (14) is modified in the following form:

$$J(\boldsymbol{\alpha}) = \sum_{i=1}^{4}\left[\int_0^{t_f} \mathbf{T}_i^T \mathbf{T}_i \, \mathrm{d}t\right] + (\mathbf{x}(t_f) - \mathbf{x}_d)^T \mathbf{M}(\mathbf{x}(t_f) - \mathbf{x}_d) \tag{23}$$

$$\mathbf{T}_i = (\dot{\boldsymbol{\delta}}_i + \boldsymbol{\omega}) \times \mathbf{h}_i \tag{24}$$

where $\mathbf{T}_i$ is an output torque vector of the ith CMG and $\dot{\boldsymbol{\delta}}_i$ is a gimbal angular velocity vector of the ith CMG in the satellite body-fixed control axes. This evaluation term for the energy consumption is derived from a new assumption of the proportional property between the output torque and the electrical energy consumption of the CMG gimbal on the basis of the reaction-wheel case [11].

Moreover, the evaluation function considers the restraint conditions of control inputs at initial and terminal times. General Earth observation satellites need a rest-to-rest maneuver, which means that the satellite body must rest at the beginning and end of the maneuver in order to observe the ground target. Then the CMG gimbals should also rest, in other words, the CMG gimbal angular velocities should be zero. The FBA is adjusted to the following restraint condition:

$$\dot{\boldsymbol{\delta}}(0) = \mathbf{0} \tag{25}$$

$$\dot{\boldsymbol{\delta}}(t_f) = \mathbf{0} \tag{26}$$

where Eq. (25) is a beginning restraint condition and Eq. (26) is an end restraint condition. These restraint conditions can be treated in the evaluation function as follows:

$$J = \sum_{i=1}^{4}\left[\int_0^{t_f} \mathbf{T}_i^T \mathbf{M}_T \mathbf{T}_i \, dt\right] + (\mathbf{x}(t_f) - \mathbf{x}_d)^T \mathbf{M}(\mathbf{x}(t_f) - \mathbf{x}_d) + \mathbf{u}^T(0)\mathbf{S}\mathbf{u}(0) + \mathbf{u}^T(t_f)\mathbf{S}\mathbf{u}(t_f) \tag{27}$$

where $\mathbf{M}_T$ is a weighting matrix of torques and normally a unit matrix. $\mathbf{S}$ is a weighting matrix that will be selected at a significantly large value. Equation (27) is the eventual evaluation function that depends on the precise energy consumption of the CMG and the restraint conditions of the control inputs. Energy-optimal paths can be precisely obtained by using the evaluation function.

B. Design of Feedback Control System

1. Limit State Feedback Control System

In this section, a feedback control system is designed in order to compensate for errors and disturbances that cannot be assumed in the path planning. The controlled object is a nonlinear system described in Eq. (8). A general linear feedback control system cannot control the present state. Therefore, the feedback control system is designed on the basis of the system's limit state feedback control logic [12].

A vector of a predicted terminal state $\mathbf{x}_{\mathrm{pre}}$, which is called a system's limit state, is described by

$$\mathbf{x}_{\mathrm{pre}}(t) = \mathbf{x}(t) + \int_t^{t_f} (\mathbf{g}(\mathbf{x}, \boldsymbol{\delta}) + \mathbf{f}(\mathbf{x}, \boldsymbol{\delta})\mathbf{u}_{\mathrm{nom}}) \, \mathrm{d}\varsigma \tag{28}$$

where $\mathbf{u}_{\mathrm{nom}}$ is a vector of the nominal inputs planned by FBA. When the system is controlled by the nominal inputs from present time t to terminal time t_f, a terminal state error vector is given in the following equation:

$$\boldsymbol{\beta}(t) = \mathbf{x}_{\mathrm{pre}}(t) - \mathbf{x}_d \tag{29}$$

The purpose of the controller design is to move the terminal state errors $\boldsymbol{\beta}$ closer to $\mathbf{0}$. The system's limit state described in Eq. (28) can be obtained by the numerical integral. A feedback control system using the system's limit state can be designed on the basis of Lyapunov analysis as follows:

$$\mathbf{u}(t) = \mathbf{u}_{\mathrm{nom}}(t) - \mathbf{F}^T(t)\mathbf{K}_p\boldsymbol{\beta}(t) \tag{30}$$

$$\mathbf{F} \equiv \frac{\partial \mathbf{g}}{\partial \mathbf{x}^T}\mathbf{f} + \frac{\partial \mathbf{g}}{\partial \boldsymbol{\delta}^T} + \left\{\frac{\partial \mathbf{f}}{\partial x_k}\mathbf{u}_{\mathrm{nom}}\right\}^{k=1,\ldots,7}\mathbf{f} + \left\{\frac{\partial \mathbf{f}}{\partial \delta_i}\mathbf{u}_{\mathrm{nom}}\right\}^{i=1,\ldots,4} \tag{31}$$

where $\mathbf{K}_p$ is a nonnegative feedback gain matrix and $\mathbf{F}$ is a newly defined matrix as will hereinafter be described in detail. This logic does not use the present state but the system's limit state $\mathbf{x}_{\mathrm{pre}}$ in the feedback controller. Therefore, this logic is effective for the nonlinear system.

2. Derivation of Control System

The feedback control system is based on the Lyapunov function that consists of the terminal state error vector $\boldsymbol{\beta}$. A scalar function V of the errors of the system's limit state is defined as a Lyapunov function by the following form:

$$V = \boldsymbol{\beta}^T\boldsymbol{\beta} \tag{32}$$

where a variation of the function V after one step Δt is described by

$$\Delta V = 2\boldsymbol{\beta}^T\Delta\boldsymbol{\beta} = 2\boldsymbol{\beta}^T\Delta\mathbf{x}_{\mathrm{pre}} = 2\boldsymbol{\beta}^T(\mathbf{F}d\boldsymbol{\delta}\Delta t) \tag{33}$$

where $\Delta\mathbf{x}_{\mathrm{pre}}$ is a variation vector of the system's limit state. The derivation of Eq. (33) is described in the next section. If $\mathbf{F}d\boldsymbol{\delta}\Delta t$ is selected to be equivalent to $-\boldsymbol{\beta}(t)$, ΔV becomes negative, and the terminal state error $\boldsymbol{\beta}(t + \Delta t)$ can be moved closer to $\mathbf{0}$. In this way, control inputs that transfer $\mathbf{x}$ to $\mathbf{x}_d$ can be obtained. If an equation $\Delta V \leq 0$ is satisfied at any time, as time advances, the system's limit state errors $\boldsymbol{\beta}$ approach $\mathbf{0}$. To satisfy the condition $\Delta V \leq 0$, the variation of the CMG gimbal angle $d\boldsymbol{\delta}$ is selected as follows:

$$d\boldsymbol{\delta} = -\mathbf{F}^T\mathbf{K}_p\boldsymbol{\beta} \tag{34}$$

Consequently, this control system can compensate for errors by modifying nominal inputs on the basis of Eq. (34). In this system, an inverse matrix of the matrix $\mathbf{F}$ cannot be assured. Therefore, the designed control logic is composed of a transposed matrix $\mathbf{F}^T$ instead of the inverse matrix $\mathbf{F}^{-1}$. The accuracy of the prediction depends on the degree of minuteness of the transition state $d\boldsymbol{\delta}$.

In an actual implementation, it may be difficult for an onboard satellite computer to predict the system's limit state with respect to computation loads. In other words, this logic might have a problem making the prediction in terms of the computation loads and the calculation time. To reduce the computation loads, the algorithm for terminal prediction was improved. If the computer does not have sufficient capacity to calculate the terminal prediction, an approximate prediction at the next step Δt may be used. The feedback control system can be reconstructed in the following form:

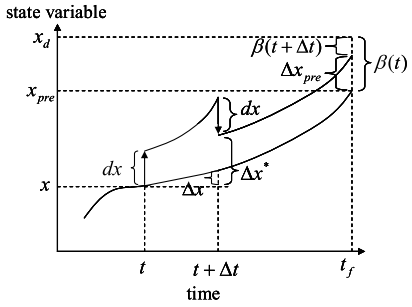

Fig. 4 Concept of the elicitation process for feedback control system.

$$\mathbf{x}_{\text{pre. lim}} = \mathbf{x}(t) + (\mathbf{g}\Delta t + \mathbf{h}(\boldsymbol{\delta}_{\text{nom}}(t) - \boldsymbol{\delta}(t))) \tag{35}$$

$$\boldsymbol{\beta}(t) = \mathbf{x}_{\text{nom}}(t + \Delta t) - \mathbf{x}_{\text{pre. lim}}(t) \tag{36}$$

where $\mathbf{x}_{\text{pre. lim}}$ is an approximate limit state in the near future and $\mathbf{x}_{\text{nom}}$ is a nominal state's trajectory. This logic achieves the reduction in computation loads by using the approximate system's limit state in the near future. On the other hand, the error of the prediction might increase, as indicated in a comparison with the previous logic using the terminal prediction.

3. Derivation of the Relation About Limit State's Variation and Present Control Inputs

This section deals with a derivation of Eq. (33) that indicates a relation between $\Delta\mathbf{x}_{\text{pre}}$ and the present control input $d\boldsymbol{\delta}$. Here, $\Delta\mathbf{x}_{\text{pre}}$ is the difference between a system's limit state predicted at present time t and that predicted at the following time $t + \Delta t$ in Fig. 4. If nominal control inputs never change after one step Δt, the system's limit state also never change and the variation $\Delta\mathbf{x}_{\text{pre}}$ becomes $\mathbf{0}$.

In Fig. 4 the state variables at the present time t are $\mathbf{x}$ and $\boldsymbol{\delta}$. At the following time $t + \Delta t$, the state variables become $\mathbf{x} + \Delta\mathbf{x}$ and $\boldsymbol{\delta} + \Delta\boldsymbol{\delta}$, where $\Delta\mathbf{x} = (\mathbf{g} + \mathbf{f}\mathbf{u}_{\text{nom}})\Delta t$ and $\Delta\boldsymbol{\delta} = \mathbf{u}_{\text{nom}}\Delta t$. The nominal input vector $\mathbf{u}_{\text{nom}}$ and the limit state's error vector $\boldsymbol{\beta}(t)$ at the present time t are equal at $t + \Delta t$.

In this paper, when Δt is sufficiently tiny, it is assumed that the variation of the limit state $\Delta\mathbf{x}_{\text{pre}}$ is linearly affected by a variation $\Delta\mathbf{x}^*$ between the present state $\mathbf{x}(t)$ and the following state $\mathbf{x}(t + \Delta t)$ in Fig. 4. Then $\Delta\mathbf{x}_{\text{pre}}$ can be evaluated, as alternated, by the state variation generated by the present control input $d\boldsymbol{\delta}$. Therefore, next, the relation between $d\boldsymbol{\delta}$ and $\Delta\mathbf{x}^*$ is derived.

The control inputs at the present time are supposed to instantly become $\boldsymbol{\delta} \to \boldsymbol{\delta} + d\boldsymbol{\delta}$. Additionally, when this transition causes the present state $\mathbf{x} \to \mathbf{x} + d\mathbf{x}$, the state variables at the present t are $\mathbf{x} + d\mathbf{x}$ and $\boldsymbol{\delta} + d\boldsymbol{\delta}$. The state variables at the following time $t + \Delta t$ become $\mathbf{x} + d\mathbf{x} + \Delta\mathbf{x}^*$ and $\boldsymbol{\delta} + d\boldsymbol{\delta} + \Delta\boldsymbol{\delta}$, where $\Delta\mathbf{x}^* = (d/dt)(\mathbf{x} + d\mathbf{x})\Delta t$ and $\Delta\boldsymbol{\delta} = \mathbf{u}_{\text{nom}}\Delta t$. Here, $\Delta\mathbf{x}^*$ can be approximately obtained by using the following Taylor expansion:

$$\begin{aligned}
\frac{d}{dt}(\mathbf{x} + d\mathbf{x}) &= \mathbf{g}(\mathbf{x} + d\mathbf{x}, \boldsymbol{\delta} + d\boldsymbol{\delta}) + \mathbf{f}(\mathbf{x} + d\mathbf{x}, \boldsymbol{\delta} + d\boldsymbol{\delta})\mathbf{u}_{\text{nom}} \\
&= \left(\mathbf{g}(\mathbf{x}, \boldsymbol{\delta}) + \frac{\partial \mathbf{g}(\mathbf{x}, \boldsymbol{\delta})}{\partial \mathbf{x}^T} d\mathbf{x} + \frac{\partial \mathbf{g}(\mathbf{x}, \boldsymbol{\delta})}{\partial \boldsymbol{\delta}^T} d\boldsymbol{\delta}\right) \\
&\quad + \left(\mathbf{f}(\mathbf{x}, \boldsymbol{\delta}) + \frac{\partial \mathbf{f}(\mathbf{x}, \boldsymbol{\delta})}{\partial \mathbf{x}^T} d\mathbf{x} + \frac{\partial \mathbf{f}(\mathbf{x}, \boldsymbol{\delta})}{\partial \boldsymbol{\delta}^T} d\boldsymbol{\delta}\right)\mathbf{u}_{\text{nom}} \\
&= (\mathbf{g} + \mathbf{f}\mathbf{u}_{\text{nom}}) + \left(\frac{\partial \mathbf{g}}{\partial \mathbf{x}^T}\mathbf{f} d\boldsymbol{\delta} + \frac{\partial \mathbf{g}}{\partial \boldsymbol{\delta}^T} d\boldsymbol{\delta}\right. \\
&\quad \left. + \frac{\partial \mathbf{f}}{\partial \mathbf{x}^T}\mathbf{f} d\boldsymbol{\delta}\mathbf{u}_{\text{nom}} + \frac{\partial \mathbf{f}}{\partial \boldsymbol{\delta}^T} d\boldsymbol{\delta}\mathbf{u}_{\text{nom}}\right) \\
&= (\mathbf{g} + \mathbf{f}\mathbf{u}_{\text{nom}}) + \mathbf{F} d\boldsymbol{\delta}
\end{aligned} \tag{37}$$

$$\Delta\mathbf{x}^* = ((\mathbf{g} + \mathbf{f}\mathbf{u}_{\text{nom}}) + \mathbf{F} d\boldsymbol{\delta})\Delta t = \Delta\mathbf{x} + \mathbf{F} d\boldsymbol{\delta}\Delta t \tag{38}$$

where the Taylor expansion abbreviates second and higher-order differential terms. This is because these terms are sufficiently small and are difficult to calculate. The term $\Delta\mathbf{x}$ in Eq. (38) is an original variation that depends on the time course and is not affected by the control input $d\boldsymbol{\delta}$. The term $\mathbf{F} d\boldsymbol{\delta}\Delta t$ in Eq. (38) is a variation term generated by the control input $d\boldsymbol{\delta}$. In this way, Eq. (33) can be derived.

IV. Verification by CMG Experimental Setup

A. Experimental Conditions

The purpose of this section is to verify the effectiveness of the designed control system with respect to the energy consumption and the safe use of CMG by comparing with the existing control system that consists of the CMG steering logic and the satellite attitude control system described in [2,13]. The proposed control system is based on the feedforward control using an energy-optimal path. In real condition, several errors and disturbances become a difficult problem. Therefore, the feedback control system is designed in order to obtain the robustness against errors and disturbances. In this study, experiments using the CMG simulated weightlessness experimental setup in Fig. 5 were carried out in order to verify the robustness under realistic conditions.

A simulated weightlessness rotating motion can be realized by using a frictionless ball bearing between the motion table and the baseplate. This device can rotate freely around the yaw axis but is constrained in the rotation about the roll and pitch axes. Therefore, in this study, it is decided that the rotational axis is the yaw axis. The CMG device shown in Fig. 5 consists of the wheel unit and the gimbal unit. Each unit has a servomotor with an encoder to detect the rotational angle. The satellite attitude and the angular velocity can be estimated by the three-axis attitude sensor mounted on the center of the motion table. Each data from the attitude sensor and the encoders is fixed through a low-pass filter to remove high-frequency noises of the data. Each device is connected to the PC through controller area network communication, and the PC controls all of the CMG units.

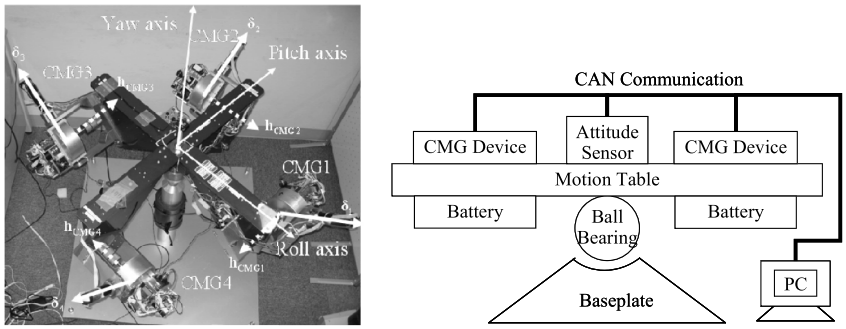

a) CMG experimental setup **b) Configuration diagram of experiment setup**

Fig. 5 CMG experimental setup and configuration diagram.

Table 1 Parameters of experiment and mission

Parameters	Symbols	Values
Inertia moment of CMG wheel	I_{CMG}	0.00354 kgm^2
Rate of CMG wheel rotation	ω_{CMG}	12000 rpm
Skew angle	β	52.0 deg
Maneuver time	t_f	20 s
Initial gimbal angles	$\boldsymbol{\delta}_0$	$[30, 90, -90, -30]$ deg
Maneuver angle	——	90 deg
Reference quaternion	——	[0, 0, 0.707, 0.707]

The parameters of the CMG experimental setup are shown in Table 1, and the inertia moment matrix of the satellite body $\mathbf{I}$ is identified by the actuation experiment as follows:

$$\mathbf{I} = \begin{bmatrix} 3.73 & 0 & 0 \\ 0 & 4.62 & 0 \\ 0 & 0 & 7.07 \end{bmatrix} \mathrm{kg \cdot m^2} \tag{39}$$

where off-diagonal elements of the inertia matrix is regarded as zero because of the difficulty in identifying it. The mission is assumed to involve a rest-to-rest attitude maneuver. It is also decided that the rotational axis of the maneuver is the yaw axis from the constraint and the insusceptibility to gravity. In this experimental setup, the roll and pitch angles can be slowly stabilized at zero angles by restoring the weak force of gravity, such as in a tumble doll that rights itself when pushed over. The maneuver is set up to the rapid and extreme condition that the existing control system using the CMG steering logic encounters a singularity problem.

B. Numerical Simulation

In this section, numerical simulations under the same condition of the experimental setup are carried out. Several parameters of the numerical simulations are shown in Table 2. Under the ideal condition, the numerical simulations with the following two logics were carried out.

Method 1: Existing control logic using the GSRInverse steering logic

Method 2: Proposed logic (feedforward control logic using the energy-optimal path)

Table 3 indicates the attitude error norms measured in $\sqrt{e_{\mathrm{roll}}^2 + e_{\mathrm{pitch}}^2 + e_{\mathrm{yaw}}^2}$, where e_i is the attitude Euler angle error around the i axis. In this study, control requirements are assumed that the terminal satellite angle error is within 1 deg and the angular velocity is within 1 deg/s. Several parameters of each control systems are selected to satisfy these control requirements. The data of the energy consumption are estimated in the following form and normalized to reform the existing logic data to 100 points:

$$\sum_{i=1}^{4}\left[\int_0^{t_f} \mathbf{T}_i^T \mathbf{T}_i \, \mathrm{d}t\right] \tag{40}$$

1. *Energy Optimality and Safe Use of CMG*

From the simulation results in Table 3, it was confirmed that the proposed logic can plan the control path that satisfies the control requirement of the terminal attitude with the same accuracy as the existing logic. Moreover, the energy consumption can be reduced by about 47% by comparing with the existing logic.

Regarding the safe use of CMG, Figs. 6 and 7 indicate that the CMG gimbal actuations of the proposed logic are smooth and the CMG gimbal angular velocity can be kept under 12 deg/s. On the other hand, the existing logic generates oscillatory behavior to avoid the singularity state and the CMG gimbal velocity reaches the limit of ± 1.0 rad/s ($= \pm 57.3$ deg/s). The results indicate that the CMG energy-optimal paths maintaining the smooth actuation can be planned by using the proposed logic, and this logic is effective for the energy consumption and the safe use of the CMG under the ideal condition.

2. *Singularity Avoidance*

This section describes how the proposed control logic can avoid singularity. Figures 6d and 7d show a manipulability that indicates a characteristics value of being in a singularity state. As shown in Fig. 6d, the CMG that is controlled by the existing logic drops into a singularity state in 5 s and moves away from the singularity state in 10 s. As shown in Fig. 7d, the CMG controlled by the proposed logic never drops into a singularity state throughout the maneuver.

The reason why the proposed logic can keep the CMG away from the singularity state is due to the following two points. The first point is that the energy consumption of the CMG is taken into consideration by the evaluation function of the path planning. The second point is that the proposed control system is not separated into an attitude controller and a CMG steering logic.

Table 2 Parameters and values of numerical simulations

Parameters	Symbols	Values
Gimbal angular velocity limit	$\dot{\boldsymbol{\delta}}_{\max}$	——
Gimbal angular acceleration limit	$\ddot{\boldsymbol{\delta}}_{\max}$	——
Parameter of steering logic	λ_0	0.1
Parameter of steering logic	m_0	0.6
Parameter of steering logic	ε_0	0.1
Parameter of steering logic	ω_s	$\pi/2$
Parameter of steering logic	ϕ_i	$0, \pi/2, \pi$
P gain of attitude control system	——	diag{6.19, 6.65, 7.66}
D gain of attitude control system	——	diag{6.80, 7.84, 10.41}
Dimension of Fourier series approximation	——	3
Basic frequency of Fourier series approximation	ω_0	$\pi/2t_f$
Weighting matrix of terminal states	$\mathbf{M}$	diag$\{5, 5, 5, 0, 50, 50, 50, 0, 0, 0, 0\} \times 10^4$
Weighting matrix of constraint condition	$\mathbf{S}$	diag$\{1, 1, 1, 1\} \times 10^6$
Uploading step size of optimization	μ	0.5

Table 3 Results of numerical simulations

	Method 1 (existing logic)	Method 2 (proposed logic)
Terminal attitude error norm, deg	0.241	0.224
Energy consumption of CMG (normalized data)	100	52.2
Maximum gimbal angular velocity, deg/s	57.30	11.04

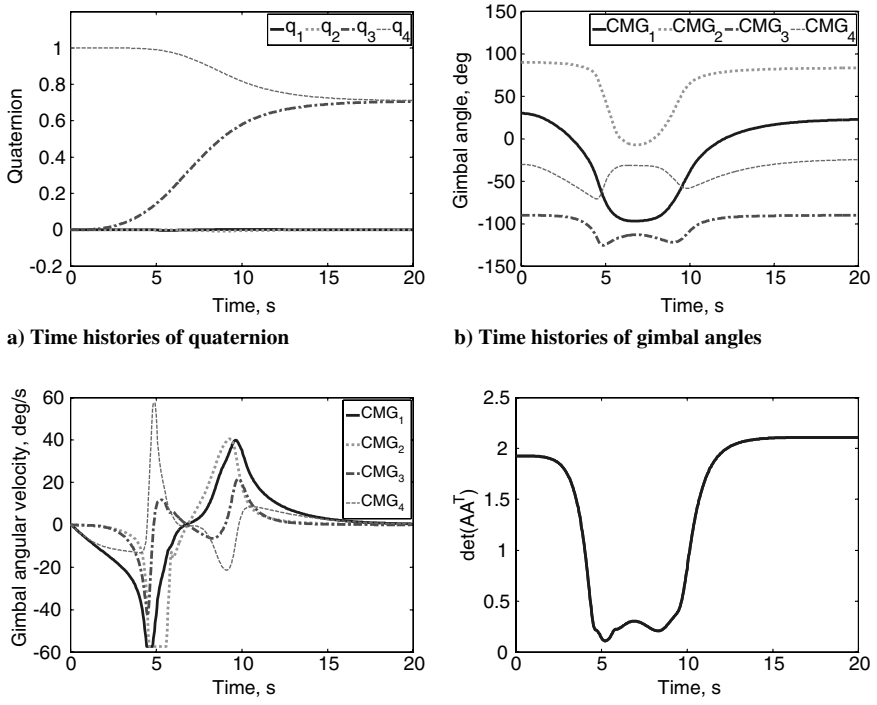

a) Time histories of quaternion **b) Time histories of gimbal angles**

c) Time histories of gimbal angular velocities **d) Time histories of manipulability**

Fig. 6 Time histories of numerical simulations (method 1).

In general, a CMG singularity state is said to be a combination of CMG gimbal angles where CMG actuation commands cannot be calculated, using a least-squares, pseudoinverse solution, to satisfy the reference torque commands from the attitude controller. In existing logics, such as the GSRInverse method, invalid actuations for the attitude control are added to a normal least-squares pseudoinverse solution in order to avoid a singularity state. However, these additional actuations have the risk of increasing the CMG energy consumption.

In the proposed logic, energy consumption is evaluated in the path planning so as to reduce the invalid actuations. Moreover, the torque command can be planned so as to maintain the effectiveness of the CMG actuation by not separating the controllers, as described previously. This property is noted from Figs. 6a and 7a. As indicated in Fig. 6, the satellite attitude controlled by the existing logic rotates around the yaw axis only because the reference maneuver is a rotation around the yaw axis. In Fig. 7, the satellite attitude controlled by the proposed logic does not rotate only around the yaw axis but

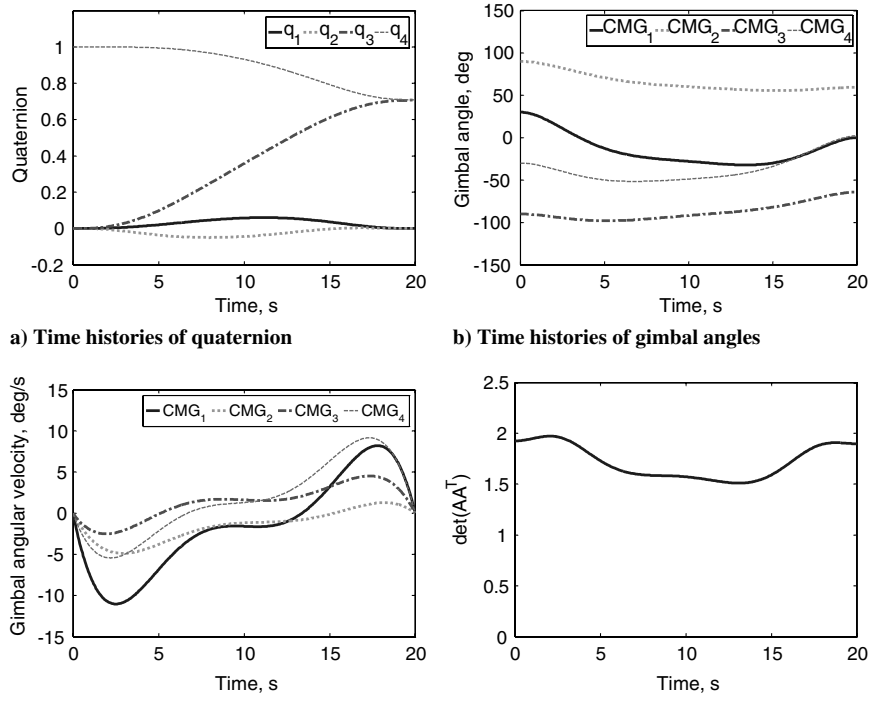

a) Time histories of quaternion **b) Time histories of gimbal angles**

c) Time histories of gimbal angular velocities **d) Time histories of manipulability**

Fig. 7 Time histories of numerical simulations (method 2).

Table 4 Parameters and values of experiments

Parameters	Symbols	Values
Control cycle	——	0.5 s
Data Sampling time	——	0.03 s
Weighting matrix of limit state feedback control	$\mathbf{K}_p$	$5 \cdot \mathbf{I}_0$
Numerical step size of terminal prediction	——	0.05 s
P gain matrix of attitude control of existing logic	——	diag{60, 60, 60}
D gain matrix of attitude control of existing logic	——	diag{105, 105, 105}

also the roll and pitch axes. This is because under the constraint of an output torque, such as a singularity state, it is not always effective for a satellite to rotate only around a reference maneuver axis. In this way, the proposed logic can plan energy effective paths that prevent the CMG from going into the singularity state.

When a commanded motion does not lead the CMG into a singularity state, it was confirmed throughout other numerical simulations that there are few differences of the control performance between the existing logic and the proposed logic.

C. Experiments Using CMG Experimental Setup

To verify the feasibility of the proposed feedback control system in an actual implementation, the experiments were carried out. Several parameters of the experiments are shown in Table 4. This experimental setup uses a high-performance computer as the controller. Therefore, the limit state feedback control system with the terminal prediction, not near future prediction, was implemented as the proposed feedback control system. The P and D gains of the attitude control system of the existing logic were selected to satisfy the other sample maneuver, a 90 deg, 20 s rest-to-rest maneuver around the yaw axis at $\boldsymbol{\delta}_0 = \mathbf{0}$. In the sample experiments, control requirements are assumed that the terminal satellite angle error is within 1 deg and angular velocity is within 1 deg/s.

In this section, experiments of the following three methods were carried out. Method 1 in Fig. 8 is the existing control system (GSRInverse steering logic), method 2 in Fig. 9 is the proposed control system (feedforward control [FF]), and method 3 in Fig. 10 is the proposed control system (feedforward control with the limit state feedback control [FF + LSFB]).

First, in order to verify the feasibility of the designed feedback control system, the results of method 2 were compared with the method 3. Second, the proposed control system was measured against the existing control system with respect to the energy consumption and the safe use of CMG by comparing the results of method 3 with the method 1.

1. *Feasibility of Designed Feedback Control System*

Figure 9a indicates that a large attitude error around the yaw axis exists at the terminal time, and the desired attitude maneuver cannot be realized by using only the feedforward control system. This is because there are some errors and disturbances that were not considered in the path planning, such as the attitude rotating friction of the ball bearing unit, the actuation delay of the CMG gimbal angular velocities, the model error of the satellite inertia, and the error of the wheel angular momentum. In particular, the results of the shortage of the satellite rotation angle indicates that the attitude rotating friction is the most difficult problem of the simulated weightlessness environment under errors and disturbances. It is difficult to solve this problem satisfactorily on Earth, but in space it can be resolved. Therefore, the satellite will be controlled by the feedforward control system more effectively in a real implementation in space than in the conditions described in this study.

Figure 10 shows the results of experiments of the feedforward control with the designed feedback controller. Figures 9a and 10a indicate that the error in the terminal attitude can be reduced by adding the designed feedback control system. The feedback control system can achieve a robust control of a nonlinear object under errors and disturbances. This is because this control system design is based

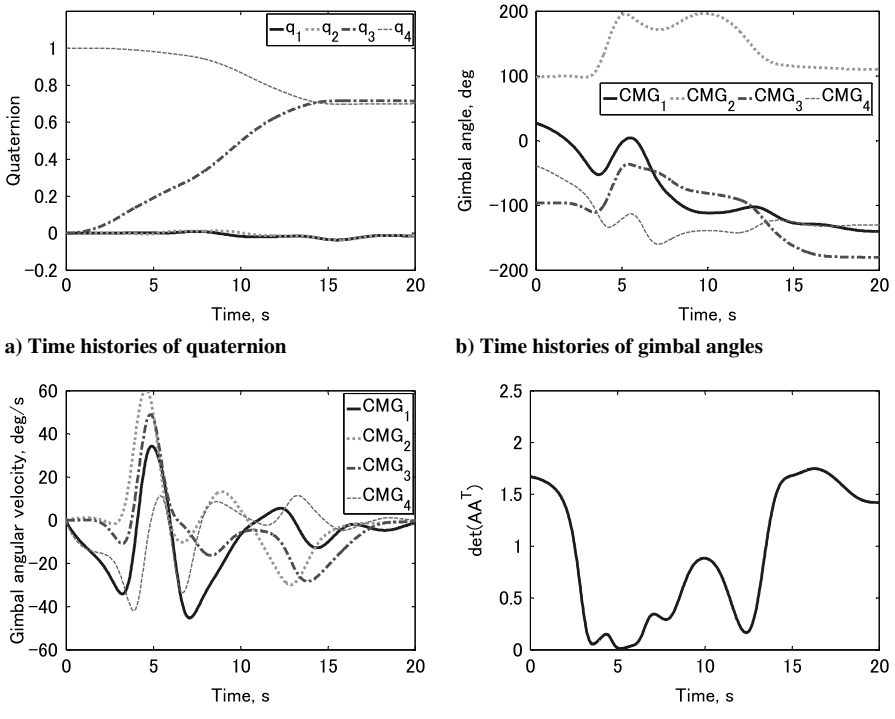

a) Time histories of quaternion **b) Time histories of gimbal angles**

c) Time histories of gimbal angular velocities **d) Time histories of manipulability**

Fig. 8 Time histories of experiment (method 1).

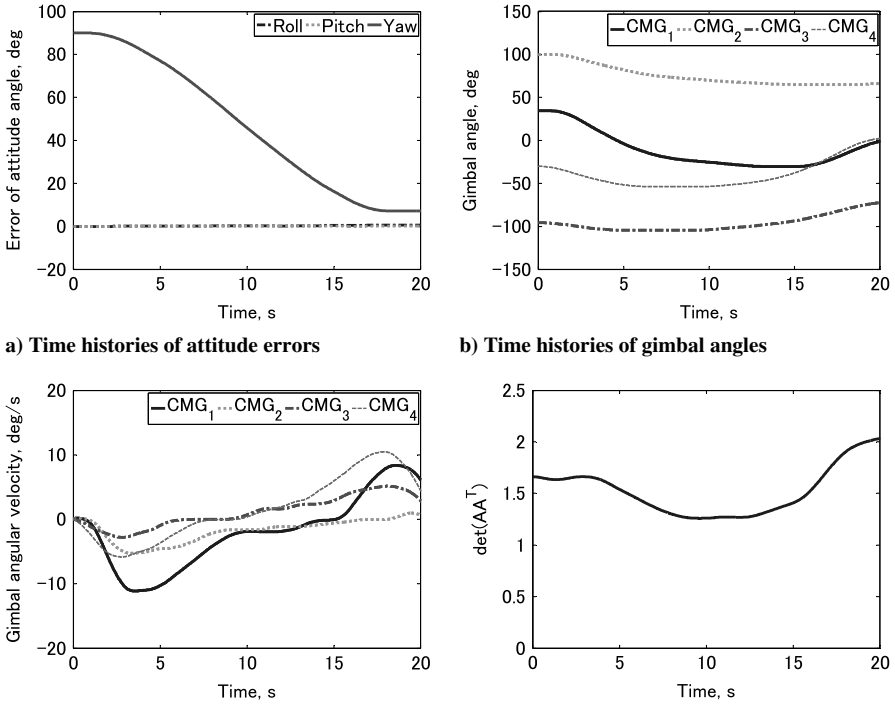

a) Time histories of attitude errors **b) Time histories of gimbal angles**

c) Time histories of gimbal angular velocities **d) Time histories of manipulability**

Fig. 9 Time histories of experiment (method 2).

on the Lyapunov function, and any present errors between reference and real state variables can be compensated for by using the state for the terminal prediction in every control cycle. However, depending on the accuracy of the terminal prediction, the designed feedback control system may not maintain the robustness if large errors exist between the ideal numerical model and the actual model. Then the model data should be uploaded, such as the satellite body inertia matrix, by using the data from identification experiments conducted in space. From the result in Fig. 10, a few attitude errors around the roll and pitch axes exist at the terminal time. It is believed that the errors are caused by the attitude determination. The attitude determination algorithm of the attitude sensor is based on the Kalman filter and numerical integrations of a gyroscope, a magnetometer, and other components. Therefore, the attitude errors around roll and pitch axes are generated by the filter error and the negative effect of the peripheral electronic devices to the magnetometer. The terminal attitude error around the yaw axis is measured as the control accuracy in Table 5.

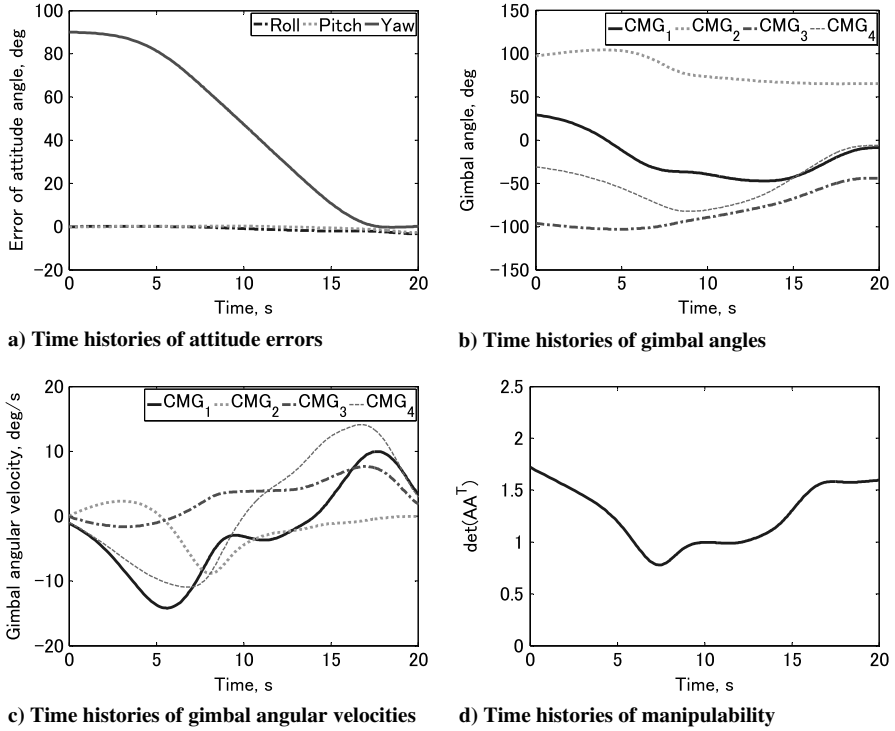

a) Time histories of attitude errors **b) Time histories of gimbal angles**

c) Time histories of gimbal angular velocities **d) Time histories of manipulability**

Fig. 10 Time histories of experiment (method 3).

Table 5 Results of experiments

Evaluation items	Method 1 (existing logic)	Method 2 (FF)	Method 3 (FF + LSFB)
Terminal Euler angle error around yaw axis, deg	0.98	6.67	0.10
Energy consumption of CMG (normalized data)	100	44.4	52.2
Maximum gimbal angular velocity, deg /s	60.54	11.13	14.19

2. Energy Consumption and Safe Use of CMG

From the results in Table 5, it was confirmed that the energy consumption of method 3 is about 47% lower than that of method 1. Moreover, the terminal error of the proposed control system is kept at a low value with the same accuracy of the existing logic. From the results, the proposed control system is more effective than the existing logic for the energy consumption of the CMG.

Regarding the safe use of the CMG, as shown in Figs. 8 and 10, gimbal angles and angular velocities of the proposed logic show the smooth actuation of the CMG. The angular velocities are kept under 15 deg /s and the trajectories of CMG gimbal angles are smooth in the whole time. On the other hand, the existing control system causes the rapid actuation that reaches the absolute maximum angular velocity of the CMG from 4 to 6 s in Fig. 8c. A relation between the rapid actuation and the singularity state can be confirmed by the manipulability time history. Figure 8d indicates that the manipulability value drops into about 0 point in the same time of the rapid actuation. The existing control system can get away from a singularity state locally by adopting the singularity avoidance logic. However, this actuation is thought to be related to the accidental failure of the CMG. From these results, the proposed control system is more effective than the existing logic for the safe use of the CMG.

3. Optimality of Energy Consumption

If a feedback control is added, the energy optimality considered in an ideal model is not guaranteed. From other numerical simulations, it was confirmed that the amount of the feedback control increases as the gap between an ideal model and the actual condition grows. Thus the CMG energy consumption also increases due to the feedback compensation, and the trajectory of the CMG deviates from the energy-optimal trajectory. When the gap is minimal, the feedback control does not work and the feedforward control can realize a reference maneuver.

In this study, the experiments were carried out under some actual gaps. Table 5 indicates that the energy consumption of method 3 was about 8% higher than that of method 2 because of the added feedback control. Method 3 maintained low the energy consumption in comparison with method 1. From these results, it is confirmed that the proposed logic with feedback control is more effective than the existing logic in terms of the CMG energy consumption.

V. Conclusions

In this paper, a new feedback control system with nominal inputs has been designed to overcome the problem of a previous control system using a CMG steering logic with respect to the energy consumption and the safe use of the CMG. The designed control system uses the nominal control inputs that had been planned on the basis of Fourier Basis Algorithm. Moreover, to acquire the robustness against several errors and disturbances in an actual implementation, a feedback controller based on the system's limit state feedback control logic is added to the designed control system. In view of CMG nonlinearity, the feedback controller uses the system's limit state, which is predicted by numerical integrals. Therefore, a satellite attitude maneuver using the CMG can be controlled effectively by the proposed logic as the whole system. From the results of the numerical simulations and the experiments using the CMG experimental setup, it was shown that the feasibility of the designed feedback control system in terms of the robustness against real errors and disturbances. The effectiveness of the proposed control system was also indicated by the experiments by comparing with the existing control logic using the CMG steering logic in terms of the energy consumption and the safe use of the CMG.

Acknowledgments

This work was supported in part by Grant in Aid for the Global Center of Excellence Program for "Center for Education and Research of Symbiotic, Safe and Secure System Design" from the Ministry of Education, Culture, Sport, and Technology in Japan.

References

[1] Wie, B., "Singularity Escape/Avoidance Steering Logic for Control Moment Gyro Systems," *Journal of Guidance, Control, and Dynamics*, Vol. 28, No. 5, Sept. 2005, pp. 948–956. doi:10.2514/1.10136

[2] Wie, B., "Singularity Robust Steering Logic for Redundant Single-Gimbal Control Moment Gyros," *Journal of Guidance, Control, and Dynamics*, Vol. 24, No. 5, Sept. 2001, pp. 865–872. doi:10.2514/2.4799

[3] Ford, K. A., and Hall, C. D., "Singular Direction Avoidance Steering for Control-Moment Gyros," *Journal of Guidance, Control, and Dynamics*, Vol. 23, No. 4, July 2000, pp. 648–656. doi:10.2514/2.4610

[4] Pechav, A. N., "Feedback-Based Steering Law for Control Moment Gyros," *Journal of Guidance, Control, and Dynamics*, Vol. 30, No. 3, May 2007, pp. 848–855. doi:10.2514/1.27351

[5] Nanamori, Y., and Takahashi, M., "Steering Law of Control Moment Gyros Using Optimization of Initial Gimbal Angles for Satellite Attitude Control," *Journal of System Design and Dynamics*, Vol. 5, No. 1, 2011, pp. 30–41. doi:10.1299/jsdd.5.30

[6] Kurokawa, H., "Survey of Theory and Steering Laws of Single-Gimbal Control Moment Gyros," *Journal of Guidance, Control, and Dynamics*, Vol. 30, No. 5, Sept. 2007, pp. 1331–1340. doi:10.2514/1.27316

[7] Kusuda, Y., Takahashi, M., and Yoshida, K., "Energy Optimal Path Planning of Satellite Attitude Maneuver Using Control Moment Gyros," 59th International Astronautical Congress, Glasgow, IAC Paper C1.8.12, 2008.

[8] Kamon, M., and Yoshida, K., "3D Attitude Control Methods of Free-Flying Dynamic System with Initial Angular Momentum," *Advanced Robotics: The International Journal of the Robotics Society of Japan*, Vol. 16, No. 2, Mar. 1998, pp. 89–97.

[9] Fernandes, C., Gurvits, L., and Li, X. Z., "Attitude Control of Space Platform/Manipulator System Using Internal Motion," *Proceedings of IEEE International Conference on Robotics and Automation*, IEEE Press, Piscataway, NJ, 1992, pp. 893–898.

[10] Nakamura, Y., and Mukherjee, R., "Nonholonomic Path Planning of Space Robots Via Bi-Directional Approach," *Proceedings of IEEE International Conference on Robotics and Automation*, IEEE Press, Piscataway, NJ, 1990, pp. 1764–1769.

[11] Endo, T., and Ueno, S., "Minimum Energy Maneuver of Satellites by Two Wheels," *Journal of the Japan Society for Aeronautical and Space Sciences*, Vol. 51, No. 598, Nov. 2003, pp. 613–620. doi:10.2322/jjsass.51.613

[12] Kamon, M., Yoshida, K., and Fukushima, R., "Orientation Control of 3D Free-Flying Robots—3rd Report: Feedback Control Methods for the Systems with Initial Angular Momentum," *Advanced Robotics: The International Journal of the Robotics Society of Japan*, Vol. 21, No. 5, Apr. 2003, pp. 75–85.

[13] Wie, B., Bailey, D., and Heiberg, C., "Rapid Multitarget Acquisition and Pointing Control of Agile Spacecraft," *Journal of Guidance, Control, and Dynamics*, Vol. 25, No. 1, Jan. 2002, pp. 96–104. doi:10.2514/2.4854